Journal of Cerebral Blood Flow & Metabolism (2013) 33, 137–145

www.jcbfm.com

ORIGINAL ARTICLE

Dynamic spatio-temporal imaging of early reflow in a neonatal rat stroke model

Pierre-Louis Leger[1,2], Philippe Bonnin[3,4], Pierre Lacombe[5], Elisabeth Couture-Lepetit[6], Sebastien Fau[1], Sylvain Renolleau[2], Abdallah Gharib[6], Olivier Baud[1,7] and Christiane Charriaut-Marlangue[1]

The aim of the study was to better understand blood-flow changes in large arteries and microvessels during the first 15 minutes of reflow in a P7 rat model of arterial occlusion. Blood-flow changes were monitored by using ultrasound imaging with sequential Doppler recordings in internal carotid arteries (ICAs) and basilar trunk. Relative cerebral blood flow (rCBF) changes were obtained by using laser speckle Doppler monitoring. Tissue perfusion was measured with [^{14}C]-iodoantipyrine autoradiography. Cerebral energy metabolism was evaluated by mitochondrial oxygen consumption. Gradual increase in mean blood-flow velocities illustrated a gradual perfusion during early reflow in both ICAs. On ischemia, the middle cerebral artery (MCA) territory presented a residual perfusion, whereas the caudal territory remained normally perfused. On reflow, speckle images showed a caudorostral propagation of reperfusion through anastomotic connections, and a reduced perfusion in the MCA territory. Autoradiography highlighted the caudorostral gradient, and persistent perfusion in ventral and medial regions. These blood-flow changes were accompanied by mitochondrial respiration impairment in the ipsilateral cortex. Collectively, these data indicate the presence of a primary collateral pathway through the circle of Willis, providing an immediate diversion of blood flow toward ischemic regions, and secondary efficient cortical anastomoses in the immature rat brain.

Journal of Cerebral Blood Flow & Metabolism (2013) **33,** 137–145; doi:10.1038/jcbfm.2012.147; published online 10 October 2012

Keywords: cerebral ischemia; collateral supply; mitochondria; oxygen consumption; reperfusion

INTRODUCTION

Perinatal arterial stroke is a cerebrovascular event occurring around the time of birth, with pathologic or radiologic evidence of focal arterial infarction mainly affecting the middle cerebral arterial (MCA) territory, with an incidence of 1 in 2,500 term births.[1] Perinatal brain injury has been associated with impaired cerebral blood flow (CBF) autoregulation to maintain blood flow with respect to arterial blood pressure. Impairment of this homeostatic mechanism has a key role in the pathophysiology of the ischemic and hemorrhagic insults in newborn brains.[2] Few studies have characterized CBF after neonatal or pediatric ischemia and hypoxia, and there is variability in reperfusion patterns reported according to the species, the developmental stage and ischemia duration.[3]

In the adult rat brain, major blood-flow reduction was observed in the ischemic core territory, when collaterals fail to provide adequate perfusion,[4] while this reduction was less marked in the surrounding penumbra.[5] Restoration of blood flow—reperfusion—to the ischemic territory was characterized by a significant hyperemia occurring immediately after occlusion release, which may be seen as a mechanism to counteract the metabolic shortage. This was followed by a postischemic hypoperfusion lasting for hours, described as the 'no-reflow phenomenon'.[6] This finding raises the question whether the relative or absolute hyperemia could also reflect blood-flow changes that occur in large vessels and in deep brain regions. To approach these questions, tissue perfusion measured by [^{14}C]-iodoantipyrine autoradiography indicated that tissues that are heavily compromised by the 2-hour period of ischemia and are destined to incur infarction show a 'relative hyperemia' during recirculation.[7]

Brain tissue perfusion has also been quantified by autoradiography in the P7 hypoxic-ischemic rat, and showed CBF in the opposite cortex remained at normal levels despite a 'hypoxia only' insult, whereas flow to the brainstem and cerebellum nearly doubled or tripled after hypoxia–ischemia (HI) in rat, respectively.[8–10] Conflicting data were reported using laser-Doppler flowmetry under normoxic resuscitation after HI in rat with increased,[11] decreased[12] and none modifications[13] of regional CBF. More recently, the spatial and temporal profiles of cortical surface CBF were analyzed in P8 mouse and P7 rat pups subjected to HI using laser speckle imaging. These authors reported that after the end of the hypoxic insult, the mean CBF level gradually increased and nearly attained its presurgical level in the ipsilateral hemisphere.[14]

To better understand whether variability in blood-flow changes evoked above were because of methodological limitations, we choose to characterize hemodynamic responses in large arteries and microvessels during early reflow in a P7 rat stroke model using a large panel of techniques. We evaluated the spatiotemporal profiles of CBF changes using 2D color-coded pulsed

[1]Sorbonne Paris Cité, INSERM U676, Univ Paris Diderot, Paris, France; [2]AP-HP, Service de Réanimation Pédiatrique, Hôpital Armand Trousseau, UPMC-Paris6, Paris, France; [3]Sorbonne Paris Cité, AP-HP, Hôpital Lariboisière, Physiologie Clinique—Explorations Fonctionnelles, Univ Paris Diderot, Paris, France; [4]Sorbonne Paris Cité, INSERM U965, Univ Paris Diderot, Paris, France; [5]Sorbonne Paris Cité, INSERM U740, Univ Paris Diderot, Paris, France; [6]Faculté de Médecine Lyon Est, CarMeN Lyon-1, INSERM U1060, Lyon, France and [7]Sorbonne Paris Cité, AP-HP, Service de Réanimation et Pédiatrie néonatales, Hôpital Robert Debré, Univ Paris Diderot, Paris, France. Correspondence: Dr C Charriaut-Marlangue, INSERM U676, Hôpital Robert Debré, 48 bd Serurier, Paris 75019, France.
E-mail: christiane.marlangue@gmail.com
The 'Fondation pour la Recherche Médicale' supported PL Leger.
Received 28 August 2012; revised 19 September 2012; accepted 19 September 2012; published online 10 October 2012

Doppler ultrasound, laser speckle contrast (LSC) imaging, and [^{14}C]-iodoantipyrine autoradiography. As decrease in blood supply leads to shortage of oxygen and mitochondrial dysfunction, we then evaluated the respiratory chain activity as an indicator of tissue metabolic state. Detailed results provided by these experiments might further our understanding on blood-flow regulation in the P7 rat brain.

MATERIALS AND METHODS

Neonatal Ischemia–Reperfusion

All experiments of this study complied with ethical guidelines of Robert Debré Hospital Research Council Review Board (A75-19-01), INSERM, and the ARRIVE guidelines (http://www.nc3rs.org/ARRIVE) and have been approved by the local ethic committee (Paris, France). Ischemia was induced in Wistar P7 rat pups (16 to 18 g; Janvier, Le Genest St-Isle, France)[15] and was adapted to isoflurane anesthesia.[16] Briefly, thermoregulated ($37.0 \pm 0.5^{\circ}$C) and anesthetized pups (1% isoflurane in O_2/N_2O (1:3)) were exposed to left middle cerebral artery electrocoagulation (MCAo) combined with a transient (50 minutes), concomitant occlusion of both common carotid arteries (CCAs). Carotid blood-flow restoration was assessed by release of the carotid clips. Sham-operated animals were only subjected to carotid artery isolation and did not receive MCAo or transient CCA occlusion (CCAo).

Physiologic Parameters

Arterial blood was collected by a PE10 catheter introduced in the femoral artery and gases (pH, Pao_2, $Paco_2$) were measured by the means of a blood-gas analyzer (Ciba-Corning 248, GMI, Inc., Ramsey, MN, USA).

Magnetic Resonance Imaging Acquisition

Pups were anesthetized by isoflurane 0.8% mixed in 30% O_2, 70% N_2 and monitored after ischemia and 10 minutes and 2 hours reperfusion ($n = 3$). During imaging, animals were thermoregulated by a water blanket heated at 37°C. Images were acquired using a 7-T horizontal MRI device (Bruker BioSpin, Rheinstetten, Germany) as previously described.[17] Diffusion-weighted images were obtained from an echo planar imaging sequence (repetition time = 3 seconds, echo time = 25 ms, *b* values = 50, 500, 1,000 s/mm^2, field of view 40 × 40 mm, matrix 256 × 256, repetitions = 3, 25 slices, thickness = 0.5 mm, duration = 9.5 minutes). The ADC (apparent diffusion coefficient) maps were computed by exponential fitting of the local signal intensity versus *b* values, using a homemade imageJ plugin (http://rsb.info.nih.gov).[17] T2-weighted images were obtained with a Rapid Acquisition with Relaxation Enhancement (RARE) sequence (repetition time = 5,404 ms, echo time values = 25.6, 76.8, 128, 179.2 ms, RARE factor = 4, field of view 40 × 40 mm, matrix 128 × 128, 25 slices, thickness = 0.5 mm, duration = 3 minutes). Animals were killed at 48 hours and coronal brain sections were stained by cresyl violet. Volumetric reconstruction was performed using a 3D imaging program (Amira, Mercury computer Systems, Inc., Chelmsford, MA, USA).

Ultrasound Imaging

Thermoregulated rat pups ($n = 6$) were subjected to ultrasound measurements under isoflurane (0.5% inhalation via a facemask in O_2/N_2O (1:3)) anesthesia using an echograph (Vivid 7, GE Medical Systems ultrasound, Horten, Norway) equipped with a 12-MHz linear transducer.[16] Heart rate and time-average mean blood-flow velocities (mBFVs) were measured in both the intracranial carotid arteries (ICAs) and the basilar trunk (BT) before surgery, during ischemia (at 40 minutes) and monitored from 1 to 15 minutes after removal of the CCAo. Heart rates were measured and reflected changes in cardiac output, as left ventricular stroke volume is quite invariable in newborns.

Laser Speckle Contrast Imaging

Imaging was performed using the full-field laser perfusion imager (Moor FLPI V3.0; Moor Instruments Ltd, Axminster, UK). Briefly, thermoregulated and anesthetized (1% isoflurane) rat pups ($n = 6$) were placed in the prone position and skin incised to provide access to the skull. Speckle images (760 × 568 pixels) were collected at 1 Hz (4 ms exposure time) and recorded in basal, after MCAo, during ischemia, during the first 20 to 30 minutes of reflow and at 24 hours. Blood-flow maps for six defined regions of interest (50 × 50 pixels each) in the penumbra were averaged and the rCBF was computed (in arbitrary units) using a 16-color palette. Changes in rCBF were expressed as a percentage of the averaged basal level.

Quantitative Measurement of Multilocal Cerebral Blood Flow

Local CBF was measured in isoflurane anesthetized P7 rat pups with the quantitative autoradiographic technique using [^{14}C]-iodoantipyrine as a diffusible tracer. Measurements were performed in sham ($n = 4$), at the end of ischemia ($n = 5$), and at 15 minutes after reperfusion ($n = 6$). The protocol followed was that adapted for the mouse,[18,19] which requires the use of a programmable infusion pump (Harvard 44) for the intravenous infusion of the tracer, so that the arterial input function was a ramp. Anesthesia was induced by 2% isoflurane progressively reduced to 1.5% inhaled via a facemask in 25% O_2 and 75% N_2. Heparin and CBF tracer were administered through a 0.3-mm (30 G) needle connected to a 500-μL Hamilton syringe through a 20-cm PE10 catheter. At the time of measurement, the infusion needle was inserted into the right jugular vein and 16 μL of heparin contained in the PE10 catheter (800 UI/kg) was slowly infused. Then, 100 μCi/kg of [^{14}C]-iodoantipyrine (ARC, American Radiolabeled Chemicals, Inc., Herts, UK, 54 mCi/mmol) diluted in 140 μL of saline was infused during 35 seconds. At the end of infusion, arterial blood was sampled by intracardiac puncture with a Myjector 300 μL (29 G needle) to determine the peak of the tracer concentration curve. Rats were then immediately decapitated and their heads were quickly frozen in isopentane chilled at -45°C.[20] Brains surrounded by the skull and cranial teguments were cut in 20 μm coronal sections and used either for autoradiography, or stained by cresyl violet. [^{14}C]-tracer concentration was assessed by densitometric analysis on autoradiograms (MCID/AIS software; InterFocus GmbH, Mering, Germany) using calibrated ^{14}C standards on the film. Absolute blood-flow values expressed in mL/min per 100 g of tissue were calculated using the local tracer concentration accumulated in brain tissue, and the tracer concentration evaluated on the basis of the cardiac plasma blood sample. Analysis of autoradiograms was performed on a total of 68 brains regions, the CBF values of which were pooled for characterizing blood-flow distribution at different caudorostral levels of the brain. The local CBF values were then calculated according to equation 5 given in Jay *et al*[18] using a brain–blood partition coefficient of 0.8.

Preparation of Isolated Mitochondria

Sham and ischemic P7 rats were killed by decapitation at the end of ischemia and at 15 minutes of reperfusion ($n = 5$ animals for each condition). The brains were then rapidly dissected out on a cold plate. Cortical tissues (corresponding to the MCA territory) were harvested from both lesioned and sham animals. Mitochondria were isolated in a 50-mmol/L Tris (pH 7.4) buffer containing 70 mmol/L sucrose, 210 mmol/L mannitol, 10 mmol/L EGTA, by differential centrifugation of cortical homogenates, as described previously[21] giving a supernatant (S2) and a mitochondrial (M1) fraction. Mitochondria were resuspended in the same medium without EGTA and kept on ice. Mitochondrial protein concentration was measured by the Bradford's method[22] using bovine serum albumin as standard.

Mitochondrial Oxygen Consumption

Mitochondrial oxygen consumption was measured using an Oxygraph (Oroboros Instrument, Innsbruck, Austria) at 25°C. Mitochondria (~0.3 mg of proteins) were incubated in 2 mL medium containing 60 mmol/L KCl, 150 mmol/L sucrose, 20 mmol/L Tris-HCl, 5 mmol/L KH_2PO_4, and glutamate 20 mmol/L at pH 7.4. Respiration state 3 was initiated by the addition of 0.2 mmol/L ADP and state 4 without ADP. The oxygen consumption was expressed in nmol O_2/min per mg of protein. The respiratory control rate (RCR) was calculated as the ratio of the state 3/state 4.

Statistical Analysis

Values are expressed as mean ± s.d. or s.e.m. ([^{14}C]-CBF values). Mean BFV between left and right ICA, and CBF values taken at five different caudorostral intervals were compared using repeated-measures ANOVA on the different groups of animals. Caudorostral profiles of CBF in reperfusion were likewise compared using repeated-measures ANOVA. *Post hoc* paired Student's *t*-test was used to analyze differences (mBFVs, interhemispheric differences in blood flow in the ipsilateral versus contralateral side of the MCAo).

RESULTS

Physiologic data indicated that P7 rat pups with a mean body weight of 17.19 ± 1.82 g had a pH of 7.32 ± 0.02, a Pa_{O_2} of 79.7 ± 12.5 mm Hg, and a Pa_{CO_2} of 62.4 ± 5.0 mm Hg in basal conditions.

Injury Produced by Ischemia–Reperfusion

Electrocoagulation of the left MCA in association with 50 minutes left and right CCAo produced a lesion in the left parietal cortex as shown on ADC (apparent diffusion coefficient) maps as early as 10 minutes after ischemia (Figure 1, upper), on T2-weighted images taken at 2 hours (Figure 1, middle) and on cresyl violet-stained sections at 48 hours (Figure 1, lower).

Dynamic Blood-Flow Monitoring During Ischemia and Early Reperfusion

During ischemia, while the two CCAs were occluded, mBFVs increased to $138 \pm 51\%$ ($n = 6$) in the BT as previously described.[16] During early reperfusion, mBFV in the BT slightly decreased to $127 \pm 32\%$ (NS versus basal values) and further remained stable. Reflow in both ICA occurred immediately after clip removing (Figures 2C to 2E). Mean BFV in the left ICA reached $63 \pm 40\%$ of basal values at 1 minute, gradually recovering to $76 \pm 21\%$ at 15 minutes. In the right ICA, one animal did not display mBFV at reperfusion (no reflow) and in the five others mBFV reached $20 \pm 11\%$ ($P < 0.001$ versus left ICA) at 1 minute and $50 \pm 33\%$ at 15 minutes ($P < 0.001$ versus left ICA, Figure 2E). Heart rates did not significantly change along the experiment (basal: 362 ± 27; ischemia: 322 ± 36; reperfusion: 357 ± 29 b.p.m.).

Representative data illustrating the pattern of blood flow before and after reperfusion using LSC imaging are shown in Figure 3. Immediately after combination of MCA and bilateral CCAo blood flow fell down (Figure 3C) in the MCA territory. After CCAo release and reflow, blood flow through superficial anastomotic arterial connections occurred between the occipital pole (supplied by the BT and posterior cerebral arteries) toward the MCA territory (Figures 3D to 3F, black arrows in Figure 3E). In the right MCA territory, LSC images (Figures 3G to 3J) showed a decrease in CBF during right CCAo (Figure 3H), and its gradual recover during early reflow (Figures 3I to 3J). The LSC images also identified venous and arterial blood flow (Figures 3K to 3N). Blood-flow recovery was gradual and incomplete during reflow in the MCA territory (Figures 3M and 3N) but observed in the terminal segment of the MCA (Figure 3N). Measures of rCBF indicated that after MCA occlusion, CBF declined to $55 \pm 8\%$, and further declined to $18 \pm 5\%$ of baseline after bilateral CCAo (Figure 3O) in the ipsilateral cortex. After bilateral CCAo release, rCBF gradually increased from $30 \pm 11\%$ at 1 minute to $44 \pm 9\%$ at 20 minutes (Figure 3O, $n = 6$) and recovered to $55 \pm 10\%$ at 24 hours (not

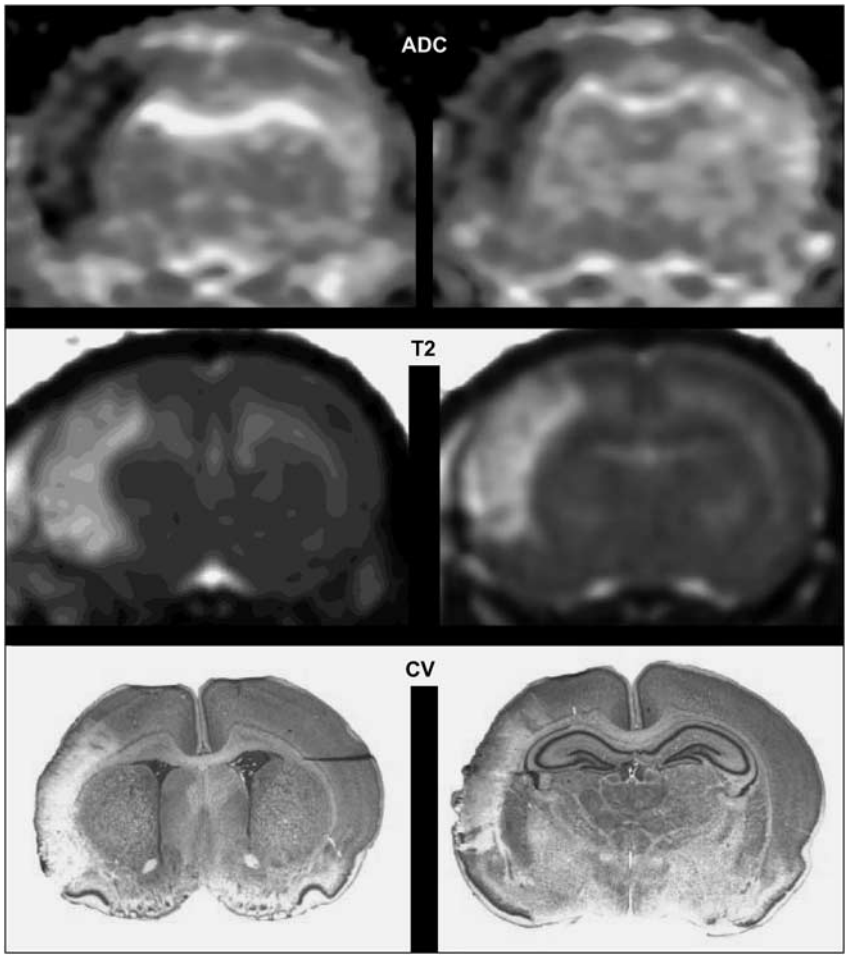

Figure 1. Ischemia–reperfusion induces cortical infarct in P7 rat brain. Upper: Representative apparent diffusion coefficient (ADC) map at 10 minutes after ischemia–reperfusion showing a cortical lesion at Bregma 1.32 and −3.24 mm, respectively. Middle: Representative T2-weighted image at 2 hours after ischemia–reperfusion showing the cortical lesion. Lower: Representative cresyl violet (CV)-stained sections from this animal at 48 hours after ischemia–reperfusion.

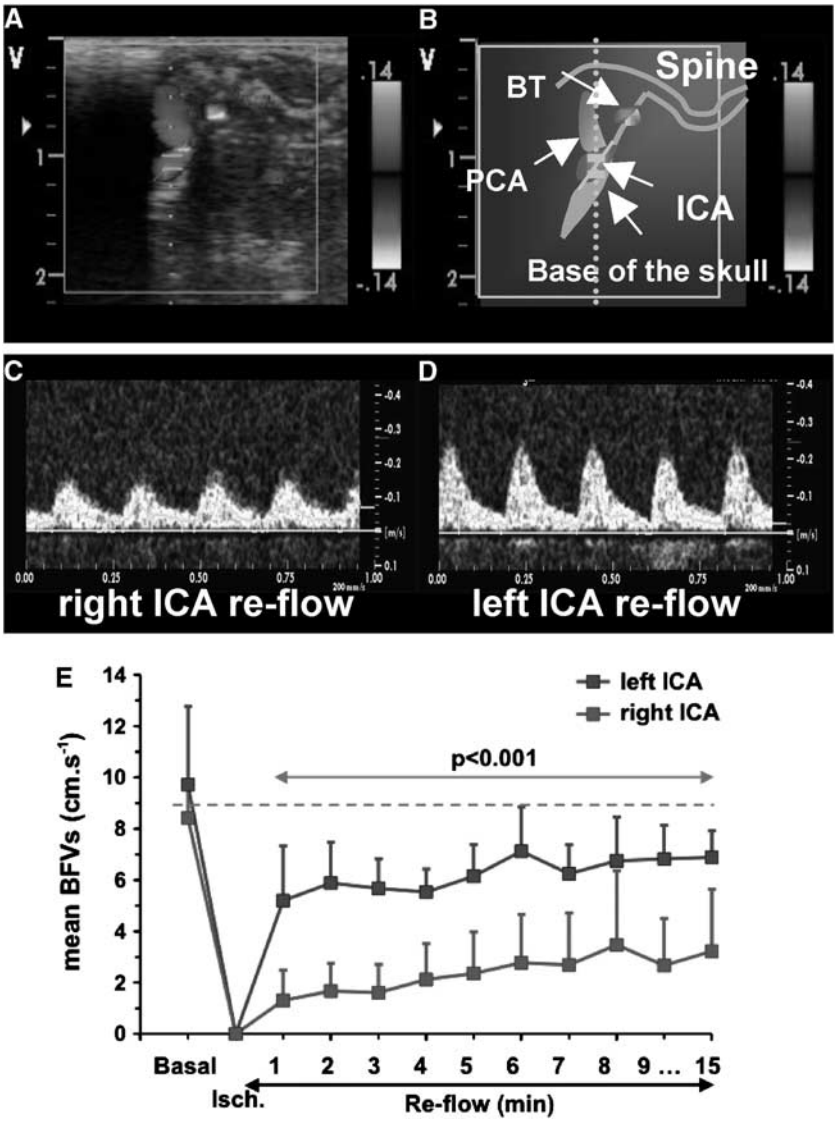

Figure 2. Time course of mean blood-flow velocities (mBFVs) in the left and right internal carotid artery (ICA) using ultrasound (US) imaging during ischemia and reflow ($n = 6$). (**A**) Para-sagittal 2D-color-coded image of brain arteries. (**B**) Schematic representation of image **A** with localization of arteries (white arrows); BT, basilar trunk; ICA, internal carotid artery; PCA, posterior cerebral artery. (**C**, **D**) Typical example of color-coded (**C**) and pulsed Doppler images in the left (**C**) and right (**D**) ICA during reperfusion. (**E**) Mean BFVs in left and right ICA were plotted in basal, during ischemia (at 40 minutes) and during the first 15 minutes of the reperfusion ($n = 6$). Note that mBFVs in the right ICA were significantly reduced as compared with values obtained in the left ICA.

shown). In the contralateral cortex, similar results were obtained with a gradually increased rCBF from $35 \pm 12\%$ at 1 minute to $48 \pm 8\%$ at 20 minutes.

Distribution of Local Cerebral Blood Flow During Ischemia and Early Reperfusion

In sham-operated rats ($n = 4$), high blood-flow values were found in brain stem regions (Figure 4A). The highest flows took place in the caudal medulla and pontic reticular formation (140 to 190 mL/100 g per minute), followed by the medial mesencephalic and diencephalic regions (110 to 130 mL/100 g per minute). The perfusion rate in cortical areas was lower ranging between 65 and 80 mL/100 g per minute, except for the piriform cortex with 100 to 115 mL/100 g per minute. Remarkably, blood flow in the trigeminal nerve was comparable to that in the medulla. Ischemia ($n = 5$) abolished perfusion (below 10 mL/100 g per minute) in the rostral two third of the brain (midbrain and forebrain). Forebrain regions of one out of five ischemic animals displayed a residual perfusion rate (15 to 25 mL/100 g per minute). Reperfusion ($n = 6$) differently attained the caudal and rostral parts of the brain. Obviously, the brain stem exhibited the highest CBF values during reperfusion, especially in its ventral part. Figures 4B and 4C provide a quantification of local CBF distribution at different caudorostral levels, and illustrate the flow gradients in the three conditions. The figure clearly showed that no postischemic hyperemia occurred in both the ipsilateral and contralateral hemibrains (Figures 4B and 4C, respectively), excepted in the medulla, pons, and cerebellum (Table 1).

Rostrocaudal Blood-Flow Profiles During Early Reperfusion

The changes in local CBF with respect to sham-operated rats at different caudorostral levels are illustrated in Figure 5. A caudorostral gradient is still present during ischemia (not shown) and reperfusion, but perfusion in ventral and medial

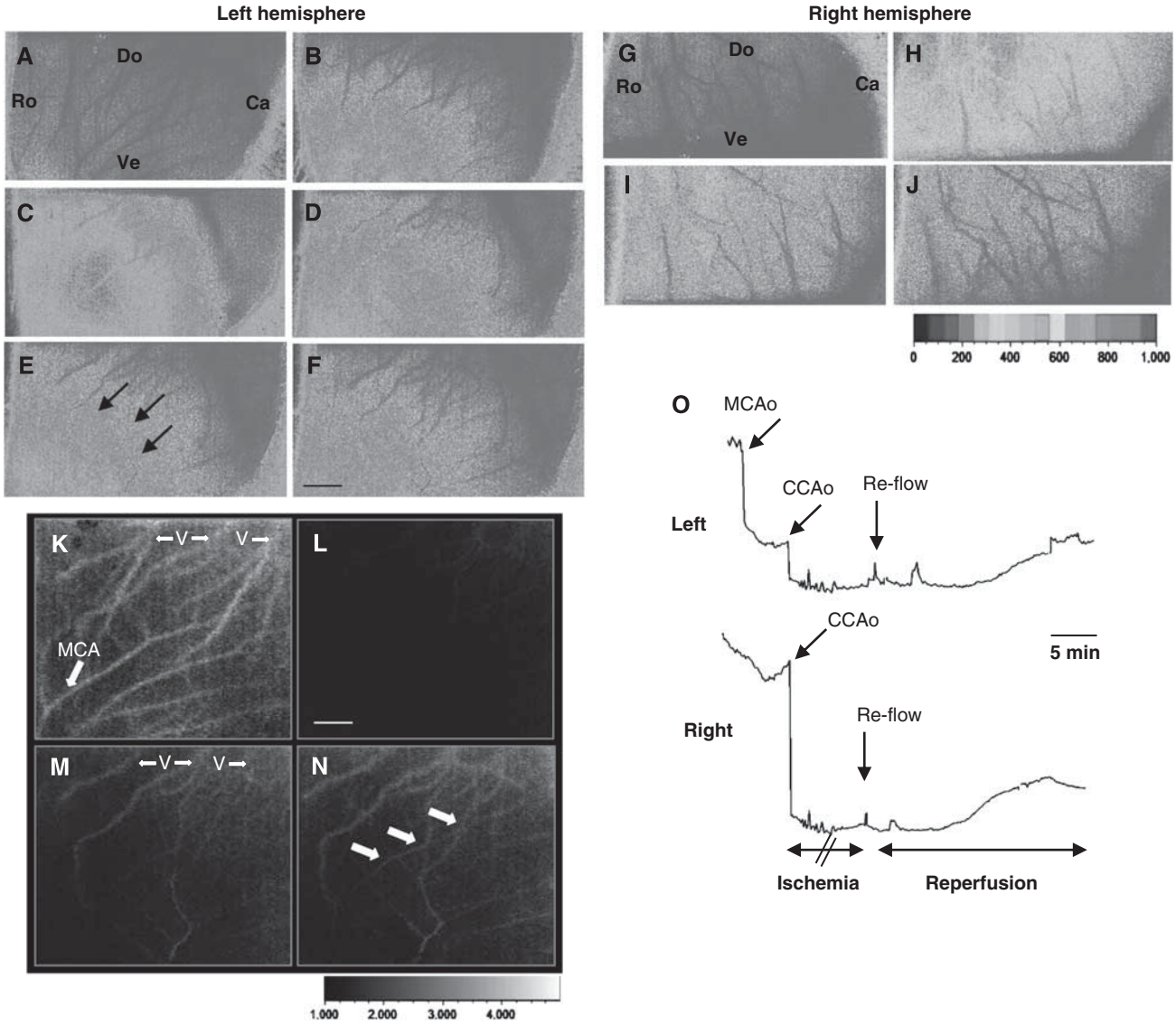

Figure 3. Typical example of spatio-temporal evolution of blood changes in the cerebral cortex in response to neonatal ischemia and reperfusion. (**A**–**F** and **K**–**N**) Laser speckle contrast (LSC) images (15 × 11 mm) in the left (**A**–**F**) and right (**K**–**N**) hemisphere are shown in basal (**A**, **K**), after middle cerebral artery (MCA) electrocoagulation (MCAo) (**B**), left and right CCA occlusion (CCAo) (**C**, **L**) and during reperfusion at 5 (**D**, **M**), 15 (**E**), and 30 (**F**, **N**) minutes. Ro, rostral; Ca, caudal; Do, dorsal; Ve, ventral. Note the expansion of the area with relative cerebral blood flow (rCBF) of ~50% of basal value (three black arrows). (**G**–**J**) LSC imaging showing blood flow in veins (V) and vessels in the cortical surface in basal (**G**), during ischemia (**H**), and during reperfusion at 5 (**I**) and 30 (**J**) minutes. Note the presence of blood flow in the terminal segment of the MCA (white arrows). (**O**) Changes in rCBF (mean of six regions of interest (ROIs) ± s.d.) in six animals subjected to ischemia–reperfusion. Upper: Representative laser-Doppler tracing in the left and right hemisphere from an ischemic animal showing perfusion deficit after MCAo and further decline after occlusion of both CCA (CCAo), and gradual reflow after CCAo release (arrow). Black scale bar represents 2 mm and white scale bar represents 1.25 mm.

regions remained less affected. This observation was substantiated in distinguishing blood flow in ventrodorsal and mediolateral regions. A detailed analysis of the results provided evidence that blood-flow decline is steeper in dorsal and lateral regions, comparatively to sham-operated rats (Figure 5). Thus, a ventrodorsal and a mediolateral blood-flow gradient are superimposed on the main caudorostral gradient.

Effects of Unilateral Occlusion of the Middle Cerebral Artery on Hemispheric Blood-Flow Distribution

The effects of unilateral occlusion of the MCA were evaluated by side-to-side differences in blood flow (Table 1). None of the interhemispheric differences observed in sham-operated and ischemic rats were significant. However, a trend to increase was observed in the ipsilateral midbrain and hindbrain of ischemic animals (Table 1). In contrast, significantly lower blood flows were found in midbrain and forebrain regions ipsilateral to the occlusion in reperfused animals. Table 1 also showed that reperfusion in ipsilateral forebrain cortical areas remained very low, with at most 20 mL/100 g per minute.

Oxidative Phosphorylation During Ischemia and Early Reperfusion

During ischemia, mitochondria isolated from ipsilateral and contralateral cortex showed a similar and significantly decreased

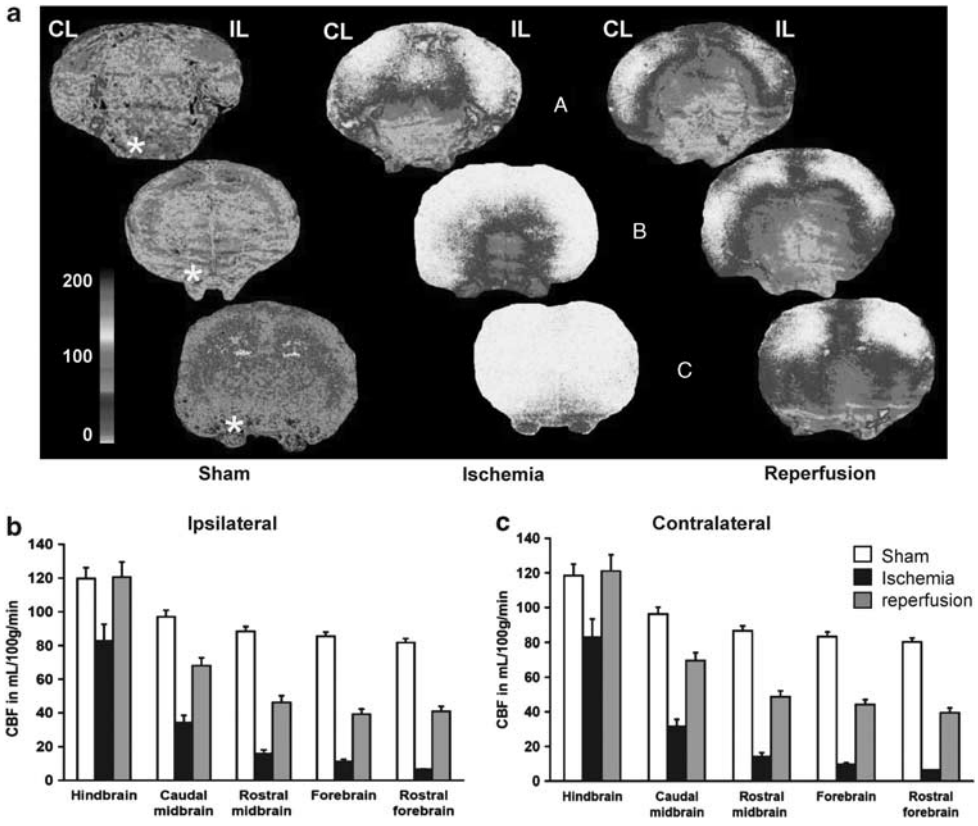

Figure 4. Cerebral blood flow (CBF) distribution in sham-operated, ischemic, and reperfused P7 rat pups. (**A**) Autoradiograms of coronal sections at three caudorostral levels (hindbrain, **a**; midbrain, **b**; forebrain, **c**) showing local tissue perfusion. The color-coded scale indicates that CBF values occasionally attained 200 mL/100 g per minute. Highly perfused regions are found in the pons and medulla, and rostrally in the ventral and medial mesencephalic brain stem and diencephalon. Lower blood-flow values are found in the lateral and dorsal cortical mantel, and in the dorsal subcortical forebrain. Remarkably, the trigeminal nerve (beneath low the brain *) clearly appears highly perfused, and somewhat preserved despite ischemia. (**B**) Blood flow at five caudorostral levels in the hemibrain ipsilateral (IL) and (**C**) contralateral (CL) to the middle cerebral artery electrocoagulation (MCAo). Absolute CBF values are decreasing in both hemibrains along a main caudorostral gradient in all conditions of perfusion, sham-operated, ischemic, and reperfused rats. A global repeated measure (RM)-ANOVA established that caudorostral blood-flow gradients are significantly different for all conditions of perfusion ($P<0.0001$). Values are mL/100 g per minute, mean ± s.e.m. for sham-operated ($n=4$), ischemic ($n=5$), and reperfused ($n=6$) P7 rats. The regions of interest are for the hindbrain the pontic and medullar reticular formation, the spinal trigeminal and vestibular nuclei, the colliculi, the cerebellum and the caudal (visual) cortex; for the caudal midbrain, the pontine and deep mesencephalic nuclei, the periaqueductal gray, the subthalamic area and hypothalamus, the lateral hippocampus, occipital (visual and auditory) and retrosplenial cortical areas; for the rostral midbrain, the thalamus, the dorsal hippocampus, the posterior parietal (somatosensory-S1 barrel field and limb, S2, and motor M1–M2) cortical areas, and the amygdala and piriform cortex; for the forebrain, the striatum, the anterior dorsal thalamus, the anterior hypothalamic area, and the anterior parietal, cingular and piriform cortical areas; and for the rostral forebrain, the caudate head, the septum, the frontal (S1-jaw and motor) cortical areas, the orbital cortex, and the olfactory tubercles and anterior olfactory nuclei.

Table 1. CBF values in the hemibrain contralateral (CL) and ipsilateral (IL) to the MCAo side in the three groups of P7 rats

Caudorostral regions	*Sham operated* (n = *4*)		*Ischemia* (n = *5*)		*Reperfusion* (n = *6*)	
	CL	*IL*	*CL*	*IL*	*CL*	*IL*
Medulla, pons, and cerebellum	129 ± 13	129 ± 13	133 ± 16	148 ± 21	164 ± 16	161 ± 15[a]
Subthalamus or colliculi[b]	117 ± 6	121 ± 6	28 ± 3	34 ± 4	84 ± 7	92 ± 5
Occipital cortex, hippocampus, thalamus	77 ± 4	78 ± 4	33 ± 4	38 ± 4	52 ± 8	34 ± 5
Parietal cortex or basal forebrain[b]	75 ± 2	78 ± 3	16 ± 2	19 ± 2	30 ± 5	18 ± 2*
Frontal cortex	82 ± 3	85 ± 3	6[c] ± 0.3	6 ± 0.3	38 ± 6	19 ± 3**

CBF, cerebral blood flow; MCAo, middle cerebral artery electrocoagulation. Values are mL/100 g per minute (mean ± s.e.m.) for the number (*n*) of rats. The regions considered belong to the five caudorostral intervals of Figure 5. As none individual interhemispheric differences in blood flow reached the level of significance, three regions displaying interhemispheric difference have been pooled for each level.
[a]$P<0.05$ versus sham values.
[b]Colliculi and basal forebrain have been considered in ischemic animal because these regions exhibited interhemispheric blood-flow differences greater than in the subthalamus and parietal cortex, respectively.
[c]The value 6 indicates background flow rate. The statistical significance of the differences between CL and IL regions of the MCAo is evaluated by bilateral *t* test.
*$P<0.05$, **$P<0.01$.

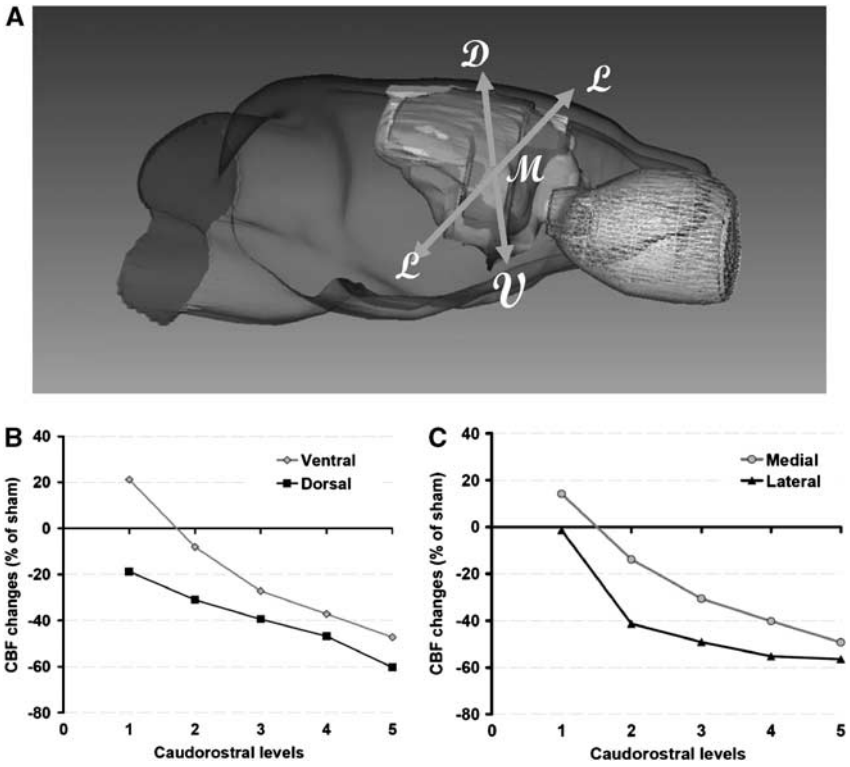

Figure 5. Regional cerebral blood flow (CBF) profiles during reperfusion. (**A**) Representative three-dimensional volumetric reconstruction from a P7 rat brain at 5 hours after ischemia (green, diffusion-weighted image; blue, T2-weighted image; yellow, eye); D, dorsal; M, medial; V, ventral; L, lateral. (**B**, **C**) Blood-flow changes are expressed in percent change of the values in the contralateral hemibrain of sham-operated rats. In each of the five rostrocaudal intervals of Figures 4B and 4C, four regions of interest were classified as ventral, dorsal, median, or lateral. Comparatively to sham-operated rats, blood-flow decline is progressively greater rostrally (RM-ANOVA, $P<0.0001$) for both the ventrodorsal (**B**) and the mediolateral (**C**) gradients.

Table 2. Oxygen consumption during phosphorylating respiration (state 3) and respiratory control ratio (RCR) in mitochondria isolated from the ipsilateral (IL) and contralateral (CL) cortex of ischemic-rat pups

	State 3	*State 4*	*RCR*
IL cortex			
Sham	18.96 ± 1.41	4.59 ± 0.35	4.13 ± 0.10
Ischemia	9.55 ± 1.33***	4.04 ± 0.33	2.38 ± 0.27***
Reperfusion	12.05 ± 1.31**	4.63 ± 0.37	2.63 ± 0.29***
CL cortex			
Sham	19.78 ± 0.97	4.75 ± 0.23	4.18 ± 0.07
Ischemia	10.98 ± 1.67**	4.00 ± 0.25	2.73 ± 0.31**
Reperfusion	16.05 ± 1.75	4.65 ± 0.22	3.43 ± 0.23

State 3 (+ ADP) and state 4 (− ADP) (in nmol O_2/min per mg protein) were measured in the mitochondrial fraction isolated from the cerebral cortex of sham P7 rats ($n=5$), ischemic rats (at the end of ischemia, $n=5$) and at 15 minutes after reperfusion ($n=5$). Data are expressed as mean ± s.e.m.; ***$P<0.001$ and **$P<0.01$ versus sham.

(∼50% of the mean sham value) state 3, complex-1-dependent phosphorylating, respiration rate and uncoupled respiration along with poorer RCR ($P<0.001$) compared with mitochondria from sham animals (Table 2). The decrease in RCR was because of a decrease in state 3 respiratory activity, while the state 4 activity did not change. At 15 minutes of reperfusion, state 3 respiratory activity in the contralateral cortex returned to values not significantly different from sham animals. In contrast, state 3 respiratory activity and RCR remained significantly reduced in the ipsilateral cortex (Table 2).

DISCUSSION

To our knowledge, this is the first study that defines arterial and multiregional CBF after cerebral stroke in the immature rat. A progressive incomplete reperfusion is depicted in the cortex during early reflow in both carotids. The gradual ipsilateral reperfusion is correlated with reduced local CBF, and reduced cortical mitochondrial respiratory function. In the contralateral hemisphere, reperfusion is also gradual with a recovery in cortical mitochondrial respiratory function. Collectively, these data indicate that the magnitude of reflow and cerebral energy metabolism after ischemia–reperfusion did not return to basal values early after reperfusion in the P7 rat, and highlight an efficient collateral network during ischemia and reperfusion.

Monitoring BFVs by using ultrasound imaging indicates no significant hyperemia over basal values in the three pre Willis large arteries. In both ICAs, reflow was potent but not maximum, and recovered to 60% to 70% within 15 minutes. Recovery became complete at 24 hours as previously reported.[23–25] The early difference in mBFVs between the left and right ICA observed at early reflow may be explained by the higher level of vasodilation reached during ischemia in the left compared with the right hemisphere, because of the upstream permanent left MCA occlusion. Conceivably, at the time of CCA's reflow, blood could reflow toward both hemispheres with the same arterial pressure, but as the vascular network is more dilated in the left side (with MCAo), blood-flow rates and BFVs reached higher values than in the right side.

Monitoring cerebral perfusion in the penumbra by laser flowmetry indicates that reperfusion in the penumbra is gradual during the first 20 minutes of reflow and reaches the level obtained with permanent MCA occlusion in some animals at 30 minutes. Studies in adult rats have shown that there is a hyperemia at the early stage of reperfusion after focal or global ischemia.[26] This hyperemia could be related to the intense vasodilation of the local vascular network, because of the delayed collateral recruitment efficient from 1 hour (or more).[27] In contrast, we do not provide evidence for such hyperemia during early reflow in rat pups. Absence of hyperemia could reflect the absence of an important vasodilation consecutive to the very early potent blood-flow redistribution though the collateral network during ischemia (efficient from a few minutes).[16] The LSC imaging has become a useful tool to map spatial and temporal dynamic changes in tissue CBF,[28] and to identify extensive anastomotic connections between cerebral arteries.[29,30] Here, we show the recruitment of anastomotic connections between distal segments of the occipital arteries (BT and PCA) and MCA at early reflow. Interestingly, recruitment of anastomotic connections between distal segments of the ACA and MCA provides immediate and persistent collateral blood flow to ischemic territories during ischemia in adult rat, but these connections disappear (anastomoses no more perfused) after spontaneous reperfusion.[29] Indeed, before reflow, flow in anastomoses follows the arterial blood pressure gradient from the vascular territory normally perfused with a good blood pressure, toward the vascular territory downstream the occluded feeding artery where the blood pressure is weak. At reflow, normalization of the blood pressure in the artery supplying the ischemic territory annuls the blood pressure gradient between the two extremities of the anastomoses, thus blood flows through itself.

Measurement of local tissue perfusion in the brain of neonates requires overcoming difficulties related to how to administer the diffusible radiotracer and to reliably evaluate tracer concentration irrigating the brain. For ischemia studies, the tracer is usually administered by intraperitoneal or subcutaneous infusion, which requires approximate estimation of the timing of the beginning and peak of the systemic tracer concentration.[9,10] The peak of the curve is measured on blood collected from the severed neck at the end of tracer infusion, and the duration of measurement is long (1 to 2 minutes). As our experimental paradigm involves a general anesthesia during CBF measurement, we circumvent the inconvenience related to approximation on the time course of tracer concentration, by infusing the tracer into the jugular vein, and measuring the peak of the arterial concentration by intracardiac puncture exactly at the end of infusion. We found that the tracer concentration measured in the cardiac blood sample was at least twice that in the severed neck blood sample. Further accuracy on the arterial tracer concentration curve was provided by the use of programmed infusion, which reproducibly produced a ramp arterial input function.[18,31] Compared with other studies, our CBF values are substantially higher than those reported in unanesthetized neonate rats.[10,31,32] Our methodological CBF procedure can hardly account for the differences, since it is very close to that of Nehlig *et al*.[31] Basal hypercapnia found in P7 rats (62.4 ± 5.0 mm Hg), compared with juvenile (36 ± 2 mm Hg) and adult rats (38 ± 1 mm Hg) could in part explained the enhanced CBF values measured in this study, because arterial CO_2 was reported to increase cerebrocortical red-cell flow under moderate isoflurane anesthesia.[33] The caudorostral gradient of blood-flow rates we found in sham-operated p7 rats is steeper than that reported in other studies.[10,31,32] Combination of isoflurane and hypercapnia would be more effective in pontic and medullar structures dedicated to vital neurovegetative functions. A detailed study of postnatal changes in local CBF in unanesthetized neonate rats showed a peak in all brain regions at P17, followed by a decrease at P21.[31] The transient increase in immature animals was suggested to reflect the high-energy demands of biosynthesis related to brain cell growth and intense myelination in subcortical white-matter structures.[31] The significantly lower blood-flow rates observed during reperfusion in the ipsilateral hemisphere can logically be ascribed to the absence of reflow by this route, as interhemispheric differences increased gradually from the caudal to the rostral territory of the MCA vascular bed, and not caudally. The very low perfusion rates in ipsilateral forebrain cortical areas also show the effect of the lack of this blood supply. In contrast, the trend in higher perfusion rates in the contralateral hemisphere of ischemic rats was more widespread in the brain, except in the rostral parts where blood flow was abolished. This trend refers to reflow originating in the BT[16] and reaching vascular beds slightly more vasodilated after ischemia on the ipsilateral side, as detected here with ultrasound Doppler records.

Mitochondrial dysfunction is the most fundamental mechanism of cell damage in cerebral HI in the developing brain.[34] However, differences are observed between HI and stroke in P7 rat brain. Indeed, at 30 minutes of reoxygenation/reperfusion the activity of the respiratory chain in mitochondria isolated from HI mice is restored, exhibiting near-normal complex-I-dependent phosphorylating respiration rates,[35] whereas such recovery is not established in our neonatal stroke rat model at 15 minutes (this study) and 30 to 40 minutes[21] after reperfusion. In contrast, respiration rates recovered in the contralateral side, although CBF recovery was still incomplete. The later data are in accordance with the particular metabolism that mediates a better tolerance to hypoxia in neonatal than in adult brain.[36] After several hours of reperfusion after HI mitochondria again exhibit a profound secondary decline in their ability to generate ATP,[37,38] known as a secondary energy failure. Previous results showed that adult rats subjected to 2 hours of focal ischemia, followed by recirculation, show an initial, partial,[39] or complete[40] recovery of mitochondrial O_2 consumption, to be followed by a gradual decrease in RCR.[39] Therefore, our data suggest that cerebral blood-flow redistribution and mitochondrial O_2 consumption differ between neonatal and adult rat during blood recirculation, and between HI and stroke (this study) in the immature brain.

In conclusion, the use of three separate techniques to evaluate blood flow in the brain during and after reperfusion in a neonatal stroke model provides useful information as each of them complements the others. Laser Speckle Flow and Laser Doppler Flow reflect red blood-cell velocity within microvessels as a measure of tissue perfusion in the brain surface, whereas color-coded pulsed Doppler ultrasound monitors red blood-cell vascular flow in the pre Willis arteries, reflecting downstream hemodynamic activity to cerebral hemispheres and more probably to deeper cerebral tissues. Blood flow autoradiography, which gives CBF in all cerebral regions, reflects tissue perfusion by blood plasma, as [^{14}C]-iodoantipyrine is a diffusible tracer. Altogether, our study highlights the strong similarity of results given by the three techniques, indicating an absence of hyperemia during early reflow according to respiration rate, and a prominent role for blood flow providing from the hindbrain and caudal midbrain supplied by the BT in an acute stroke model in the P7 rat. Gradual reperfusion found in the ipsilateral hemisphere also appeared to be fairly well correlated with impaired RCR.

DISCLOSURE/CONFLICT OF INTEREST

The authors declare no conflict of interest.

REFERENCES

1 Badve CA, Khanna PC, Ishak GE. Neonatal ischemic brain injury: what every radiologist needs to know. *Pediatr Radiol* 2012; **42**: 606–619.
2 Pryds A, Tønnesen J, Pryds O, Knudsen GM, Greisen G. Cerebral pressure autoregulation and vasoreactivity in the newborn rat. *Pediatr Res* 2005; **57**: 294–298.

3 Manole MD, Foley LM, Hitchens TK, Kochanek PM, Hickey RW, Bayir H *et al.* Magnetic resonance imaging assessment of regional cerebral blood flow after asphyxial cardiac arrest in immature rats. *J Cereb Blood Flow Metab* 2009; **29**: 197–205.
4 Liebeskind DS. Understanding blood flow: the other side of an acute arterial occlusion. *Int J Stroke* 2007; **2**: 118–120.
5 Girouard H, Iadecola C. Neurovascular coupling in the normal brain and in hypertension, stroke, and Alzheimer disease. *J Appl Physiol* 2006; **100**: 328–335.
6 Siesjo BK. Measurements of cerebral oxygen consumption: advantages and limitations. *Eur Neurol* 1981; **20**: 194–199.
7 Tsuchidate R, He QP, Smith ML, Siesjo BK. Regional cerebral blood flow during and after 2 hours of middle cerebral artery occlusion in the rat. *J Cereb Blood Flow Metab* 1997; **17**: 1066–1073.
8 Ringel M, Bryan RM, Vannucci RC. Regional cerebral blood flow during hypoxia-ischemia in the immature rat: comparison of iodoantipyrine and iodoamphetamine as radioactive tracers. *Brain Res Dev Brain Res* 1991; **59**: 231–235.
9 Mujsce DJ, Christensen MA, Vannucci RC. Cerebral blood flow and edema in perinatal hypoxic-ischemic brain damage. *Pediatr Res* 1990; **27**: 450–453.
10 Vannucci RC, Lyons DT, Vasta F. Regional cerebral blood flow during hypoxia-ischemia in immature rats. *Stroke* 1988; **19**: 245–250.
11 Ioroi T, Yonetani M, Nakamura H. Effects of hypoxia and reoxygenation on nitric oxide production and cerebral blood flow in developing rat striatum. *Pediatr Res* 1998; **43**: 733–737.
12 Thiringer K, Hrbek A, Karlsson K, Rosén KG, Kjellmer I. Postasphyxial cerebral survival in newborn sheep after treatment with oxygen free radical scavengers and a calcium antagonist. *Pediatr Res* 1987; **22**: 62–66.
13 Fabian RH, Perez-Polo JR, Kent TA. Perivascular nitric oxide and superoxide in neonatal cerebral hypoxia-ischemia. *Am J Physiol Heart Circ Physiol* 2008; **295**: H1809–H1814.
14 Ohshima M, Tsuji M, Taguchi A, Kasahara Y, Ikeda T. Cerebral blood flow during reperfusion predicts later brain damage in a mouse and a rat model of neonatal hypoxic-ischemic encephalopathy. *Exp Neurol* 2012; **233**: 481–489.
15 Renolleau S, Aggoun-Zouaoui D, Ben-Ari Y, Charriaut-Marlangue C. A model of transient unilateral focal ischemia with reperfusion in the P7 neonatal rat: morphological changes indicative of apoptosis. *Stroke* 1998; **29**: 1454–1460, discussion 1461.
16 Bonnin P, Leger PL, Deroide N, Fau S, Baud O, Pocard M *et al.* Impact of intracranial blood-flow redistribution on stroke size during ischemia-reperfusion in 7-day-old rats. *J Neurosci Methods* 2011; **198**: 103–109.
17 Fau S, Po C, Goyenvalle C, Meric P, Charriaut-Marlangue C. Do early MRI signals predict lesion size in a neonatal stroke rat model? *AJNR Am J Neuroradiol* advance online publication, 3 May 2012 (e-pub ahead of print).
18 Jay TM, Lucignani G, Crane AM, Jehle J, Sokoloff L. Measurement of local cerebral blood flow with [^{14}C]iodoantipyrine in the mouse. *J Cereb Blood Flow Metab* 1988; **8**: 121–129.
19 Joutel A, Monet-Leprêtre M, Gosele C, Baron-Menguy C, Hammes A, Schmidt S *et al.* Cerebrovascular dysfunction and microcirculation rarefaction precede white matter lesions in a mouse genetic model of cerebral ischemic small vessel disease. *J Clin Invest* 2010; **120**: 433–445.
20 Greenberg JH, LoBrutto C, Lombard KM, Chen J. Postmortem diffusion of autoradiographic blood flow tracers. *Brain Res* 1999; **842**: 184–191.
21 Leger PL, De Paulis D, Branco S, Bonnin P, Couture-Lepetit E, Baud O *et al.* Evaluation of cyclosporine A in a stroke model in the immature rat brain. *Exp Neurol* 2011; **230**: 58–66.
22 Bradford MM. A rapid and sensitive method for the quantitation of microgram quantities of protein utilizing the principle of protein-dye binding. *Anal Biochem* 1976; **72**: 248–254.
23 Bonnin P, Sabaa N, Flamant M, Debbabi H, Tharaux PL. Ultrasound imaging of renal vaso-occlusive events in transgenic sickle mice exposed to hypoxic stress. *Ultrasound Med Biol* 2008; **34**: 1076–1084.
24 Villapol S, Bonnin P, Fau S, Baud O, Renolleau S, Charriaut-Marlangue C. Unilateral blood flow decrease induces bilateral and symmetric responses in the immature brain. *Am J Pathol* 2009; **175**: 2111–2120.
25 Bonnin P, Debbabi H, Mariani J, Charriaut-Marlangue C, Renolleau S. Ultrasonic assessment of cerebral blood flow changes during ischemia-reperfusion in 7-day-old rats. *Ultrasound Med Biol* 2008; **34**: 913–922.
26 Gao X, Ren C, Zhao H. Protective effects of ischemic postconditioning compared with gradual reperfusion or preconditioning. *J Neurosci Res* 2008; **86**: 2505–2511.
27 Liebeskind DS. Collateral circulation. *Stroke* 2003; **34**: 2279–2284.
28 Dunn AK, Bolay H, Moskowitz MA, Boas DA. Dynamic imaging of cerebral blood flow using laser speckle. *J Cereb Blood Flow Metab* 2001; **21**: 195–201.
29 Armitage GA, Todd KG, Shuaib A, Winship IR. Laser speckle contrast imaging of collateral blood flow during acute ischemic stroke. *J Cereb Blood Flow Metab* 2010; **30**: 1432–1436.
30 Paul JS, Luft AR, Yew E, Sheu FS. Imaging the development of an ischemic core following photochemically induced cortical infarction in rats using Laser Speckle Contrast Analysis (LASCA). *Neuroimage* 2006; **29**: 38–45.
31 Nehlig A, Pereira de Vasconcelos A, Boyet S. Postnatal changes in local cerebral blood flow measured by the quantitative autoradiographic [^{14}C]iodoantipyrine technique in freely moving rats. *J Cereb Blood Flow Metab* 1989; **9**: 579–588.
32 Lyons DT, Vasta F, Vannucci RC. Autoradiographic determination of regional cerebral blood flow in the immature rat. *Pediatr Res* 1987; **21**: 471–476.
33 Lee JG, Smith JJ, Hudetz AG, Hillard CJ, Bosnjak ZJ, Kampine JP. Laser-Doppler measurement of the effects of halothane and isoflurane on the cerebrovascular CO2 response in the rat. *Anesth Analg* 1995; **80**: 696–702.
34 Ten VS, Starkov A. Hypoxic-ischemic injury in the developing brain: the role of reactive oxygen species originating in mitochondria. *Neurol Res Int* 2012; **2012**: 542976.
35 Niatsetskaya ZV, Sosunov SA, Matsiukevich D, Utkina-Sosunova IV, Ratner VI, Starkov AA *et al.* The oxygen free radicals originating from mitochondrial complex I contribute to oxidative brain injury following hypoxia-ischemia in neonatal mice. *J Neurosci* 2012; **32**: 3235–3244.
36 Simpson IA, Carruthers A, Vannucci SJ. Supply and demand in cerebral energy metabolism: the role of nutrient transporters. *J Cereb Blood Flow Metab* 2007; **27**: 1766–1791.
37 Gilland E, Puka-Sundvall M, Hillered L, Hagberg H. Mitochondrial function and energy metabolism after hypoxia-ischemia in the immature rat brain: involvement of NMDA-receptors. *J Cereb Blood Flow Metab* 1998; **18**: 297–304.
38 Ten VS, Yao J, Ratner V, Sosunov S, Fraser DA, Botto M *et al.* Complement component c1q mediates mitochondria-driven oxidative stress in neonatal hypoxic-ischemic brain injury. *J Neurosci* 2010; **30**: 2077–2087.
39 Kuroda S, Katsura KI, Tsuchidate R, Siesjo BK. Secondary bioenergetic failure after transient focal ischaemia is due to mitochondrial injury. *Acta Physiol Scand* 1996; **156**: 149–150.
40 Rehncrona S, Mela L, Siesjo BK. Recovery of brain mitochondrial function in the rat after complete and incomplete cerebral ischemia. *Stroke* 1979; **10**: 437–446.